External Magnetic Field Assisted Synthesis of Snow-Flake Like Cobalt Fractals and Dimension analysis

[1]Mahdiyar Bagheri, [2]Anuraj Sundararaj, [3]Gopalakrishnan Chandrasekaran, [4]Helen Annal Therese, [5]Tejabhiram Yadavalli

Nanotechnology Research Center, SRM University, Kattankulathur - 603203, Tamilnadu, India
Email: jarunaraj@gmail.com

[Received: 13 November, 2014; Accepted: 8th December, 2014]

Abstract — Snow-flake like cobalt fractals structures was synthesized by the reduction of cobalt chloride using hydrazine hydrate as the reducing agent. Syntheses were performed in the presence of manifold external magnetic field. The structural, crystallographic and magnetic properties of the synthesized materials were studied. Change in morphology of the synthesized nanostructure with the external magnetic field was observed. To study the change in geometry of cobalt fractals, a new method for studying the fractal dimensions has been employed. It was observed that the cobalt fractal size and dimensions proportionally increase with the external magnetic field. The preferred crystal growth orientation of the fractals were observed to vary in both hcp and fcc Co phases, with the field strength of the applied external magnetic field. The cobalt fractals were found weakly ferromagnetic compared to the reported bulk and nano counterpart.

I. INTRODUCTION

Magnetic nanomaterials have received significant attention in the past two decades due to their wide range of application like data storage, spintronic and bio-medical devices [1-4]. Cobalt is a well known ferromagnetic material with distinct properties like high saturation magnetization, high coercivity and structure dependent magnetic and electronic properties [5]. Efforts have been focused on synthesising cobalt nanowires, nanorods and nanoparticles using different synthesis methods. The synthesis methods are classified into chemical reduction, polyol process, and thermal decomposition of organometallic precursor, thermolysis and hydrothermal/solvo-thermal [6-17]. Each of these methods has specific parameters which allow one to control the nucleation, growth mechanism, crystal structure, shape and size of nanostructures. Compared to nanostructures like rods and wires, special agglomerated morphologies like snowflakes, cauliflowers and hollow spheres have not received significant attention. Research has been limited to the following growth parameters - precursor type, reducing agents, concentration, temperature, and pH [18]. In this paper we report on the effect of magnetic field as external parameter in the synthesis of cobalt snowflake-like fractals. The relationship between the properties of the synthesized cobalt nanostructures and the effect of external magnetic field employed was investigated by field emission scanning electron microscope (FESEM), x-ray diffractometer (XRD) and vibrating sample magnetometer (VSM). In order to investigate the change in the geometry of cobalt snowflake-like fractals, the FESEM images were analysed by a new method based on box counting (that uses image pixels to calculate the dimension).

II. EXPERIMENTAL

Set up

The schematic of the experimental setup is shown in Fig.1. In this experiment the magnetic field employed for the synthesis of cobalt nanostrucutures was ensured to be homogenous in the area of the synthesis by using a proper beaker size. The first step of the experiment was to place a small beaker containing the reaction mixture between the poles of an electromagnet with a large flat surface. Variable DC current source and gauss meter were used to control and measure the magnetic field intensity between the poles of the electromagnet.

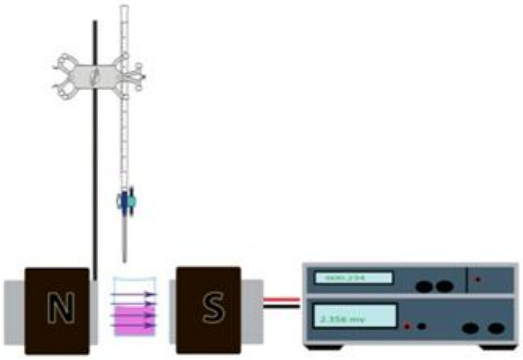

Fig. 1. Schematic representation of the experimental set up

Synthesis

The precursor solution was prepared by dissolving 1 gram of cobalt chloride into 20 ml of ethanol. A solution of the reducing agent was prepared by adding 1 gram of sodium hydroxide into 20 ml of hydrazine hydrate solution. The two solutions were mixed together in a beaker and placed in-between the poles of an electromagnet. The reaction was performed without any stirring. All the reactions were conducted at room temperature and atmospheric pressure.

The above experiments were repeated with varying magnetic fields (0 G, 200 G, 400 G, 600 G, and 800 G) for 48 hours. The formation of a mirror like metallic cobalt layer on the walls of the beaker was observed after the completion of the reaction. The product was then centrifuged and washed with DI water followed by ethanol and dried at 70 ^{o}C for 12 hours. The dried samples were then characterized by FEI's Quanta FEG 200 FESEM to study the particle size and morphology. The crystallinity of the sample was studied by PAN Analytical X-Pert Pro powder XRD and its magnetic properties were studied using a Lakeshore 7410 VSM.

III. RESULTS AND DISCUSSION

The formation mechanism of the cobalt nanostructures during the synthesis in external magnetic field is given below.

$$CoCl_2.6H_2O + CH_3CH_2OH + N_2H_4.H_2O + 2NaOH$$
$$\downarrow$$
$$Co + N_2 + 7H_2O + 2H_2 + 2NaCl + CH_3CH_2OH$$

Fig. 2. (a-f) show the FESEM images of all the synthesized cobalt nanostructures. Fig. 2 (a, b) show the FESEM images of the sample synthesized at O G. Fig. 2. (a) shows the presence of two different kinds of cobalt structures, rods and snowflake-like fractals. Rod shaped structures have a size range of 0.5 to 40 μm in length and a diameter of 2 to 5.5 μm. When observed at a higher magnification (Fig. 2 (b), it is clear that these rod like structures are made up of twisted fractals. When the intensity of the external magnetic field was increased from 0 to 800G, the rod shaped structures became less prominent and the structures formed were found to be snowflake-like, as shown in Fig. 2 (a-f). This change in geometry can be explained by the random motion of seed particles or building units in the liquid reaction medium. The random motion causes the building units to face magnetic field lines at different contact angles and consequently they become magnetized in different directions. The result of random motion to preferable crystallographic growth orientation leads to growth and agglomeration of building units in all three dimensions.

The most interesting structure found in the synthesized samples is the snowflake-like cobalt fractals. As shown in Fig. 3 (a-e), fractals are formed in all five experimental conditions. Fractals are produced by the aggregation of similar building units with different scale. The perfect snowflake structure shown in Fig. 3 (a) has six handles and single fractal handle is shown in Fig. 3 (b).

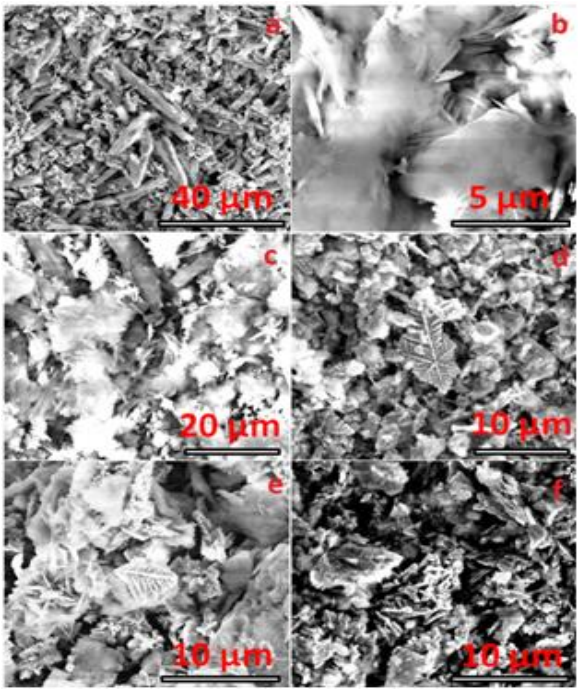

Fig. 2. FESEM images of cobalt nanostructures a, b) synthesized at 0 G, c, d, e, f) synthesized at 200, 400, 600 and 800 G, respectively

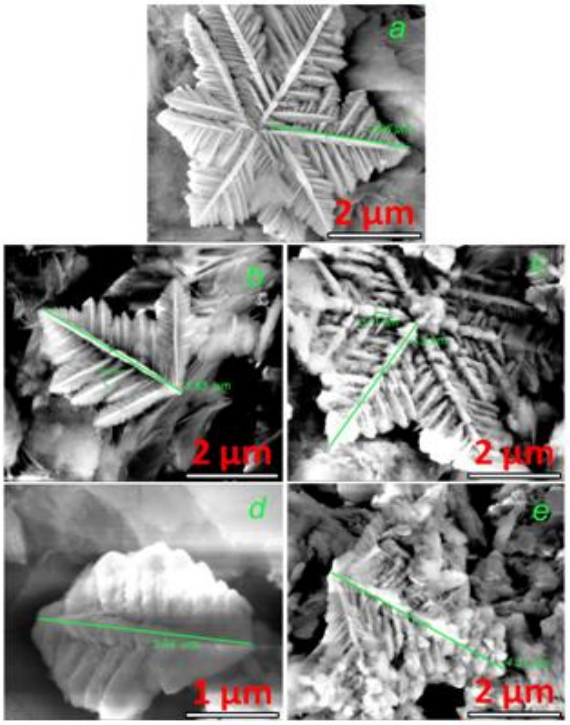

Fig. 3. (a-e) SEM images of snow flake like cobalt fractal structures at higher magnification at 0, 200, 400, 600 & 800 G, respectively

The fractals in sample made at 0 G and 200 G have almost similar shape with handle length of 2.8 to 3.6 μm as shown in Fig. 3 (a, b). Unlike the minute and gradual changes seen in the structure of the fractals between 0 and 200 G, large and sudden changes in the morphology of fractals were seen between 200 and 400 G. The fractals became large in sample synthesized at 400 G. When the intensity of the magnetic field was increased the change in appearance of the fractals, from a structures with sharp edges to big blunt structures was observed. The cobalt sample synthesized at 800 G was observed to have many agglomerated cobalt particles as shown in Fig 3 (e).

XRD Studies:

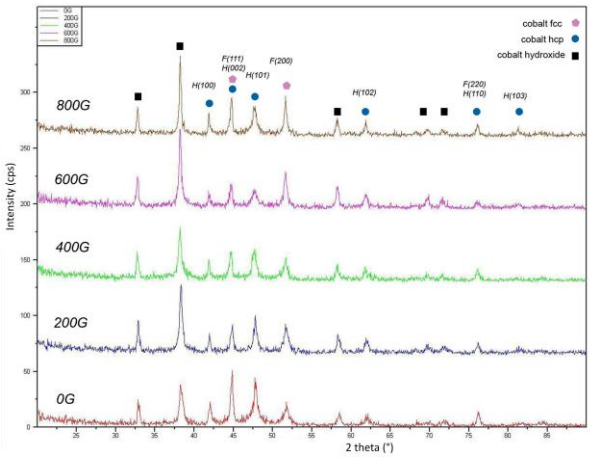

Fig. 4. XRD patterns of cobalt nanostructures synthesised in different magnetic fields

Fig. 4 shows the XRD patterns of cobalt nano structures prepared in different magnetic fields. The XRD studies was carried out with Cu-kα source (λ=0.154 nm) in the 2θ range of 20 - 90°, operated at 45 kV and 40 mA tension. The XRD patterns showed polycrystalline cobalt in hcp and fcc crystal structures along with the existence of cobalt hydroxide phase. The highest peak intensity in XRD patterns (2θ=38.31°) belongs to that of cobalt hydroxide. The presence of cobalt hydroxide in samples could be the result of a high pH medium used for the synthesis and drying of the product at atmospheric condition. The intensity of cobalt hydroxide peaks were observed to increase in the samples synthesized at higher intensity magnetic fields. This suggests that the magnetic field limits the cobalt metal formation and increased the chance of hydroxide formation. The cobalt peaks were not sharp and were found to have low intensity with different crystal orientations. This is expected for polycrystalline cobalt synthesized at room temperature. According to XRD profiles, the intensity of the peaks in 2θ position 44.806° and 47.800° referring to hcp (002) and hcp (101) crystal orientation decreased in samples synthesized in higher magnetic fields. On the other hand, the peak at 2θ=51.730° corresponding to fcc (200) is seen to increase in samples which were synthesized in higher magnetic fields. The change in the intensity of these peaks suggests that the growth orientation of the polycrystalline metallic cobalt nanostructure is influenced by the external magnetic field.

Fractal dimension analysis:

To analyze the observed changes in the morphology of fractal structures formed at 0 to 800 G, it is necessary to use the common universal parameter for the characterization of fractal agglomeration, known as the fractal dimension 'D'. Generally fractals have complicated shape and non integer dimension. The method which was employed to analyze the fractal dimension is based on the digital image processing of two dimensional pictures and box counting. In the original box counting method, the grid consists of p_i^2 squares drawn over the fractal image. $n(p_i)$ determines the number of squares required to cover the entire fractal. The next step consists of choosing finer and finer grids ($p_1^2<p_2^2<\ldots$) and counting the corresponding numbers of squares covering the image ($n(p_1)...n(p_m)$). Fractal dimensions were obtained by calculating the asymptotic slope in the double logarithmic plot of $n(p_i)$ versus $1/p_i$. In this work, we used the pixels of the FESEM image as individual units of the grid. The fractal images were distinguished clearly from their surroundings using the 'mask color' technique. The two dimensional image of the fractal was then stored in the form of two dimensional arrays of pixels, where the non-zero (black) pixels correspond to the area occupied by the fractals and zero (white) pixels correspond to the unoccupied area. By increasing the number of pixels in unit area of the image, we obtained finer and finer grids. The remaining steps are similar to any typical box counting method. The following calculation is for the sample synthesized at 200 G.

In the first step, the FESEM image, having a resolution of 200 pixels/cm^2 of the sample synthesized at 200 G was obtained. Then a fractal was clearly distinguished from the background by the use of contrasting colors. The fractal structure is left in grayscale, while the background is colored blue as shown in Fig. 5 (a). By masking gray scale pixels into black, as shown in Fig. 5 (b), the number of black pixels or boxes needed to cover the entire fractal structure can be counted. Box counting was done by using 'Digital Image processing' software. This procedure has been used for the same image at different resolutions of 400, 600, 800 and 1000 pixels/cm^2.

The box count of fractal area 'A' and the root of total number of pixels (maximum length of the fractal) 'L' for same image at different resolutions are shown in Table. I. The 'D' for each image at different resolutions was then calculated by the general relation:

$$D = \frac{\text{Ln A}}{\text{Ln L}} \quad \ldots\ldots (2)$$

The value of the average fractal dimension for the sample synthesized at 200 G is 1.836 which was calculated by

finding the average value of calculated fractal dimensions.

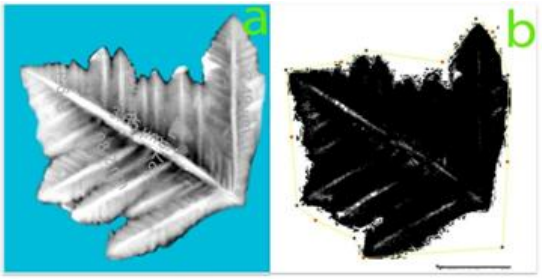

Fig. 5. Processed SEM images of snow flake like cobalt fractal structures synthesized at 200 G, a) Separating fractal from background, b) Masking grayscale color (separation and counting the number of pixels has been done by using 'Digital Image processing' software)

Table .1. Calculated numbers of pixels and fractal dimension for sample synthesized at 200 G

Resolution(pixels per cm^2)	200	400	600	800	1000
A	885	1752	2625	3453	4325
L	201311	770250	1734115	3070019	4792491
Calculated fractal dimension	1.799	1.814	1.824	1.833	1.837

The calculated results of average fractal dimensions for all samples are shown in Table. II. Snow flake-like cobalt structures in all the samples have fractal dimension less than 2. Results obtained for samples 0 and 200 G have almost similar fractal dimension of 1.827 and 1.836. The calculated average fractal dimension varied from 1.827 in 0 G sample to 1.954 in 800 G sample. The change in fractal dimension was observed to be proportional to the increase in magnetic field. A graph of magnetic field vs. the fractal dimension is shown in Fig. 6 (a). It can be noted from the graph that the proportionality between external magnetic field employed and the calculated average fractal dimension is linearly increasing. The linear increase in fractal dimension is noted to be predominant in the samples synthesized in the magnetic fields of intensities – 200 G and 400 G.

Table. II. Calculated average fractal dimensions for sample synthesized from 0-800 G

Resolution ⇨ / sample ⇩		200	400	600	800	1000	Calculated average fractal dimension
0G	A	895	1796	2674	3539	4388	1.827
	L	223530	890768	2014402	3567419	5792421	
200G	A	885	1752	2625	3453	4325	1.836
	L	201311	770250	1734115	3070019	4792491	
400G	A	1031	2062	3080	4063	5088	1.870
	L	404004	1607161	3588506	6392966	96973247	
600G	A	1041	2079	3112	4153	5204	1.927
	L	615802	2456206	5525935	9761032	15435648	
800G	A	764	1555	2362	3075	3864	1.954
	L	430986	1707043	3845643	6861369	10712216	

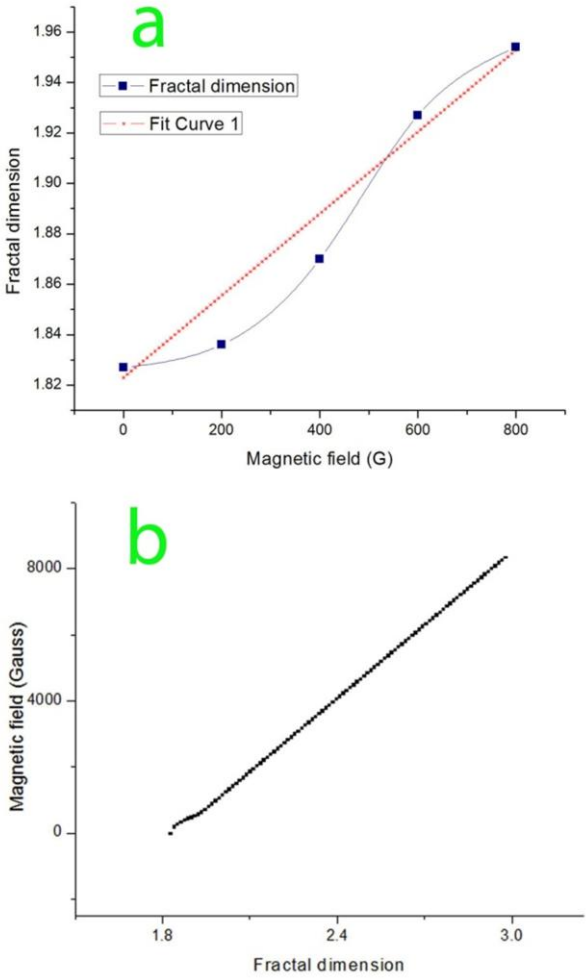

Fig .6. a) Change in fractal dimension with respect to magnetic field, b) Extrapolation of the graph between fractal dimension and magnetic field strength

A graph signifying the change in fractal dimension with external magnetic field was drawn. The external magnetic field required to synthesize cobalt fractal structures with a fractal dimension greater than 2 were predicted by extrapolating the graph. Fig. 6 (b) shows the extrapolated graph by logarithm fitting method. The graph predicts that an approximate external magnetic field of 2×10^3 G is required for obtaining a dimension greater than 2 and 8×10^3 G for 3. However, the influence of different variable parameters governs the growth mechanism, so the derived assumption based on the extrapolation of the graph is not precise or complete to be applied directly.

VSM study:

The magnetic measurement was carried out on samples synthesised at 200 G – 400 G in which sudden change in the agglomeration geometry and fractal dimension was seen. The ferromagnetic hysteresis loops of the sample, given in Fig. 7 (a-b), shows retentivity values of 11.70 emu/g and 14.32 emu/g. Coercivity in the samples

synthesized at 200 G and 400 G were observed to be 550.04 G and 602.25 G respectively.

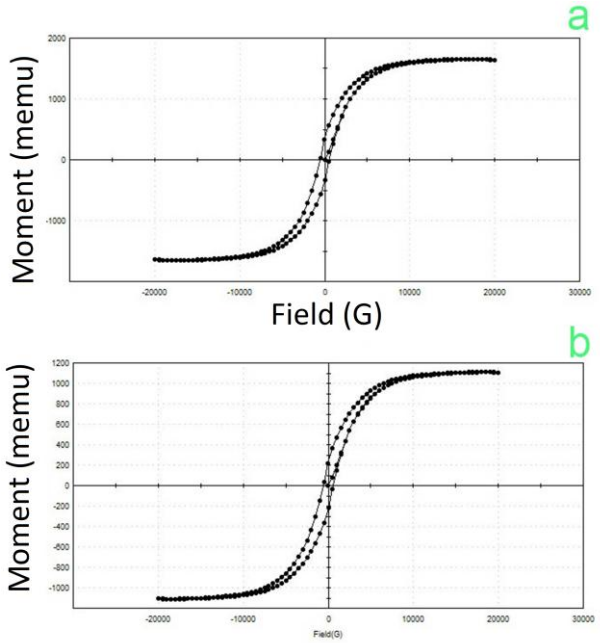

Fig.7. VSM results of (a) 200 G and (b) 400 G sample at room temperature

These values are much higher than coercivity measured for both cobalt at the bulk scale (a few tens of Oe [20]) and micrometer size cobalt fibres (100-350 Oe) [21]. The reason for this difference can be attributed to the shape anisotropy of snowflake-like cobalt structures. It can also be attributed to magneto-crystalline anisotropy, as a result of the change of crystal growth orientation of hcp and fcc phase, with increase in intensity of the magnetic fields. In comparison with the cobalt at the bulk scale (168 emu/g) [22] and micrometre cobalt fibres reported (139 emu/g) [23], the magnetic saturation of samples (59-74 emu/g) were found to be dramatically reduced which can be attributed to the presence of cobalt hydroxide in samples.

From the observed results we can hypothesize the relationship between growth of the fractals and their crystal structure. At 0 G and 200 G the influence of the magnetic field on the formation of cobalt fractal is minimal and hence an equal amount of rod like and fractal like cobalt is seen. As the external field increases, the formation of fractals is favored over that of rods. This results in the formation of bulky fractals with increased dimensions. Likewise, the appearance of fcc and hcp phases is observed at 0 G, whereas the planes peaks corresponding to the fcc phase increases with the increase in the external magnetic field. From the VSM study results, we can deduce that the fractals have ferromagnetic property, although their magnetic saturation is very weak compared to other Co nanostructures that has been reported.

IV. CONCLUSION

The Cobalt fractals were synthesised in the presence of varying external magnetic fields. A new method for the characterization of fractal dimension was used successfully to determine the dimension and area of the fractals, using the resolution of FESEM images. The samples showed proportionality in fractal dimension with the intensity of the employed magnetic field. The reduction in quantity of rod shape geometry in samples indicates the multidirectional influence of magnetic field on growth of cobalt microstructure. The influence of the external field also dominates crystal structure and magnetic properties. Increase in the plane peaks of cobalt fcc phase was observed along with the decrease in plane peaks of hcp phase, when the intensity of the external magnetic field was increased. The prepared cobalt samples show ferromagnetic behaviour but weak saturation magnetization in comparison with cobalt structures reported earlier.

V. ACKNOWLEDGEMENT

The authors thank SRM University and Dr. T. R. Pachamuthu for providing the facilities to carry out this part of work.

VI. REFERENCES

[1]. A.B. Bourlinos, A. Bakandritsos, V. Georgakilas and D. Petridis, “Surface Modification of Ultrafine Magnetic Iron Oxide Particles”, Chem. Mater. vol. 14, pp. 3226–3228, July 2002.

[2]. L. Josephson, J. Manuel Perez and R. Weissleder, “Magnetic Nanosensors for the Detection of Oligonucleotide Sequences”, Angew. Chem. Int. Ed. Vol. 40, pp. 3204–3206, Sep 2001.

[3]. Y.W. Jun, Y.M. Huh, J.S. Choi, J.H. Lee, H.T. Song, S. Kim, S. Yoon, K.S. Kim, J.S. Suh and J. Cheon, “Nanoscale size effect of magnetic nanocrystals and their utilization for cancer diagnosis via magnetic resonance imaging”, J Am Chem Soc. vol. 127, pp. 5732-5733, Apr 2005.

[4]. S. Sun, C.B. Murray, D. Weller, L. Folks and A. Moser, “Monodisperse FePt nanoparticles and ferromagnetic FePt nanocrystal superlattices”, Science. 17; vol. 287, pp. 1989-1992, Mar 2000.

[5]. I.H.J. Arellano, J. Mangadlao, I.B. Ramiro, K.F Suazo, “3-component low temperature solvothermal synthesis of colloidal cadmium sulfide quantum dots”, Materials Letters. Vol. 64, pp. 785-788, Mar 2010.

[6]. X. Zhang, C. An, S. Wang, Z. Wang and D. Xia, "Green Synthesis of Metal Sulfide Nanocrystals Through a General Composite-Surfactants-Aided-Solvothermal Process", J. Cryst. Growth. Vol. 311, pp. 3775–3780, Jul 2009.

[7]. Q. Xia, X. Chen, K. Zhao and J. Liu, "Synthesis and characterizations of polycrystalline walnut-like CdS nanoparticle by solvothermal method with PVP as stabilizer", Mater. Chem. Phys. Vol. 111, pp. 98–105, Sep 2008.

[8]. M. Charterjee and A. Patra "Cadmium Sulfide Aggregates through Reverse Micelles", J. Am. Ceram. Soc. vol. 84, pp. 1439–1444, Dec 2004.

[9]. R.B. Khomane, A. Manna, A.B. Mandale and B.D. Kulkarni, "Synthesis and characterization of dodecanethiol -capped cadmium sulfide nanoparticles in a winsor II microemulsion of diethyl ether/AOT/water" Langmuir. vol. 18, pp. 8237-8240, Sep 2002.

[10]. J. Zhang, L. Sun, C. Liao, and C. Yan, "Size control and photoluminescence enhancement of CdS nanoparticles prepared via reverse micelle method," Solid State Communications, vol. 124, pp. 45–48, Sep 2002.

[11]. B.A. Simmons, S. Li, V.T. John, G.L. Mcpherson, A. Bose, W. Zhou and J. He, "Morphology of CdS nanocrystals synthesized in a mixed surfactant system", Nano Lett. Vol. 2, pp. 263–268, Apr 2002.

[12]. M. G. Guzmán, J. Dille and S. Godet, "Synthesis of silver nanoparticles by chemical reduction method and their antibacterial activity", J Chem Biomol Eng. Vol. 2, pp. 104-111, 2009.

[13]. D. Kim, S. Jeong and J. Moon, "Synthesis of silver nanoparticles using the polyol process and the influence of precursor injection", Nanotechnology. Vol. 17, article ID. 4019, July 2006.

[14]. Y. K. Jung , J. I. Kim and J.K. Lee, "Thermal Decomposition Mechanism of Single-Molecule Precursors Forming Metal Sulfide Nanoparticles", J. Am. Chem. Soc. vol. 132, pp. 178–184, Dec 2009.

[15]. C. Erk, M. Y. E. Yau, H. Lange, C. Thomsen, P. Miclea, R. B. Wehrspohn, S. Schlecht and M. Steinhart, "Formation of gold nanoparticles in polymeric nanowires by low-temperature thermolysis of gold mesitylene", J. Mater. Chem. vol. 22, pp. 684-690, Nov 2011.

[16]. Hiromichi Hayashi, and Yukiya Hakuta, "Hydrothermal Synthesis of Metal Oxide Nanoparticles in Supercritical Water", Materials. vol. 3, ISSN No. 3794-3817, Jun 2010.

[17]. A. Singh, R. Kumar, N. Malhotra and Suman, "Preparation of ZnO nanoparticles by solvothermal process", International Journal for Science and Emerging Technologies with Latest Trends". vol. 4, pp. 49-53, Dec 2012.

[18]. Sunil Pandey, Goldie Oza, Ashmi Mewada and Madhuri Sharon, "Green Synthesis of Highly Stable Gold Nanoparticles using Momordica charantia as Nano fabricator", Arch. Appl. Sci. Res. vol. 4, pp. 1135-1141, 2012.

[19]. N. Soni and S. Prakash, "Factors affecting the geometry of silver nanoparticles synthesis in Chrysosporium Tropicum and Fusarium Oxysporum", Am. J. Nanotechnol. vol. 2, pp. 112-121, 2011.

[20]. D. A. van Leeuwen, J. M. van Ruitenbeek, L. J. de Jongh, A. Ceriotti, G. Pacchioni, O. D. Häberlen, and N. Rösch, "Quenching of Magnetic Moments by Ligand-Metal Interactions in Nanosized Magnetic Metal Clusters", Phys. Rev. Lett. vol. 73, pp. 1432, Sep 1994.

[21]. Amel Dakhlaoui, Leila S. Smiri, Gerard Babadjian, Frederic Schoenstein, Philippe Molinie and Noureddine Jouini, "Controlled Elaboration and Magnetic Properties of Submicrometric Cobalt Fibers", J. Phys. Chem. C. vol. 112, pp. 14348–14354, Jun 2008.

[22]. G. Dumpich, T. P. Krome and B. Hausmans, " Magnetoresistance of single Co nanowires", J. Magn. Magn. Mater. pp. 248, 241, Jul 2002.

[23]. J. Vidal, J. Rivas and M.A. López Quintela. "Synthesis of monodisperse maghemite nanoparticles by the microemulsion method.", Colloids and Surfaces A: Physicochem. Eng. Aspects. vol. 288, pp. 44-51, October 2006.

◈◈◈